

## Electronic Supplementary Information

### Morphology does not matter: WSe<sub>2</sub> Luminescence Nanothermometry Unravelled

Paloma Martínez-Merino,<sup>a</sup> Miguel A. Hernandez-Rodríguez,<sup>b,c</sup> José C. Piñero,<sup>d</sup> Carlos D.S. Brites,<sup>c</sup> Rodrigo Alcántara,<sup>a</sup> and Javier Navas<sup>a</sup>

<sup>a</sup>Departamento de Química Física, Facultad de Ciencias, Universidad de Cádiz, E-11510 Puerto Real, Cádiz, Spain.

<sup>b</sup>Departamento de Física, Universidad de La Laguna, Apdo. Correos 456, E-38200 San Cristóbal de La Laguna, Santa Cruz de Tenerife, Spain

<sup>c</sup>Phantom-g, CICECO – Aveiro Institute of Materials, Department of Physics, University of Aveiro, 3810-193 Aveiro, Portugal.

<sup>d</sup>Departamento de Didáctica (Área de Matemáticas), Universidad de Cádiz, E-11510 Puerto Real, Spain.

I.	Structural Characterization.....	2
II.	Spectroscopic Characterization .....	3
III.	Thermal characterization.....	5
	<i>Fit parameters of the thermal calibration curves for the samples.</i> .....	5
	Survey on relative thermal sensitivity and temperature uncertainty in TMDCs, quantum dots and nanowires samples.....	7
	Variation of the photoluminescence with temperature .....	5
IV.	References .....	8

## I. Structural Characterization

The quantum dots in sample **1** were between 3-11 nm in size with an average of  $4 \pm 1$  nm.

In sample **2**, the nanostructures were rod-shaped with a length of  $18 \pm 5$  nm and a diameter of  $4 \pm 1$  nm. The distribution of particle sizes found in both samples follows a log-normal trend whose curve fits the function:

$$y = \frac{A}{\sqrt{2\pi} w x} \exp\left(-\left(\ln\left(\frac{x}{x_c}\right)\right)^2/(2w^2)\right) \quad (\text{Eq. S1})$$

Table S1 shows the fit parameters for the size of sample **1** and for the length and diameter of sample **2**.

**Table S1.** Size distribution from TEM images presented in Figure 1. The OriginLab software was used to fit the curve given by Eq. S1 to experimental datapoints.

Sample	Parameter	Value	Units
<b>1</b>	$A$	$51 \pm 3$	$\text{nm}^{-1}$
	$w$	$0.24 \pm 0.02$	
	$x_c$	$5.4 \pm 0.1$	nm
	$r^2$	0.94	
<b>2</b> (length)	$A$	$200 \pm 15$	$\text{nm}^{-1}$
	$w$	$0.30 \pm 0.03$	
	$x_c$	$17.3 \pm 0.5$	nm
	$r^2$	0.89	
<b>2</b> (diameter)	$A$	$55 \pm 7$	$\text{nm}^{-1}$
	$w$	$0.34 \pm 0.06$	
	$x_c$	$4.1 \pm 0.2$	nm
	$r^2$	0.63	

**Table S2.** Size distribution from DLS presented in Figure 3. The OriginLab software was used to fit the curve given by Eq. S1 to experimental datapoints.

Sample	Parameter	Value	Units
<b>1</b>	$A$	$458 \pm 5$	$\text{nm}^{-1}$
	$w$	$0.15 \pm 0.01$	
	$x_c$	$31.3 \pm 0.1$	$\text{nm}$
	$r^2$	0.997	
<b>2</b>	$A$	$1850 \pm 54$	$\text{nm}^{-1}$
	$w$	$0.182 \pm 0.007$	
	$x_c$	$124 \pm 1$	$\text{nm}$
	$r^2$	0.991	

The expected interplanar distance of a hexagonal  $P6_3/mmc$  lattice can be calculated by using Eq. S2:

$$\frac{1}{d_{hkl}^2} = \frac{4(h^2 + hk + k^2)}{3\left(\frac{a^2}{a^2}\right)} + \frac{l^2}{c^2} \quad (\text{Eq. S2})$$

## II. Spectroscopic Characterization

The UV-Vis spectra of samples 1 (QDs) and 2 (NRs) are shown in Figure S1. Note that sample 2 absorbs in the range between 300 and 400 nm, while the range for sample 1 is slightly higher, extending up to 500 nm.

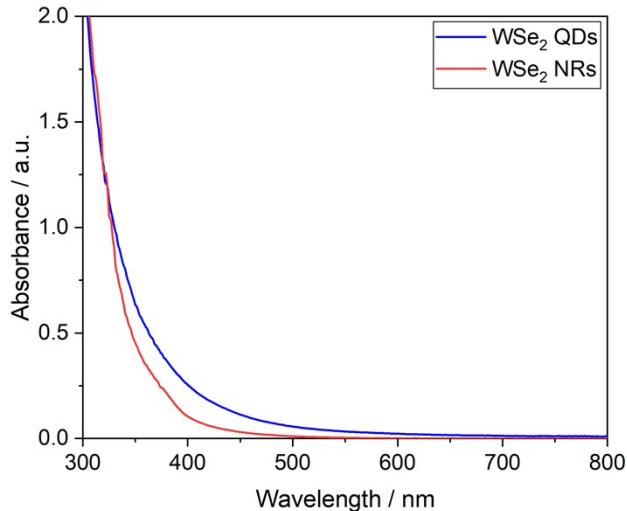


**Figure S1.** UV-VIS absorbance registered for the samples prepared.

In Figure S2, the excitation spectra for samples **1** and **2** clearly demonstrate their excitation capability within the UV-VIS spectral range.

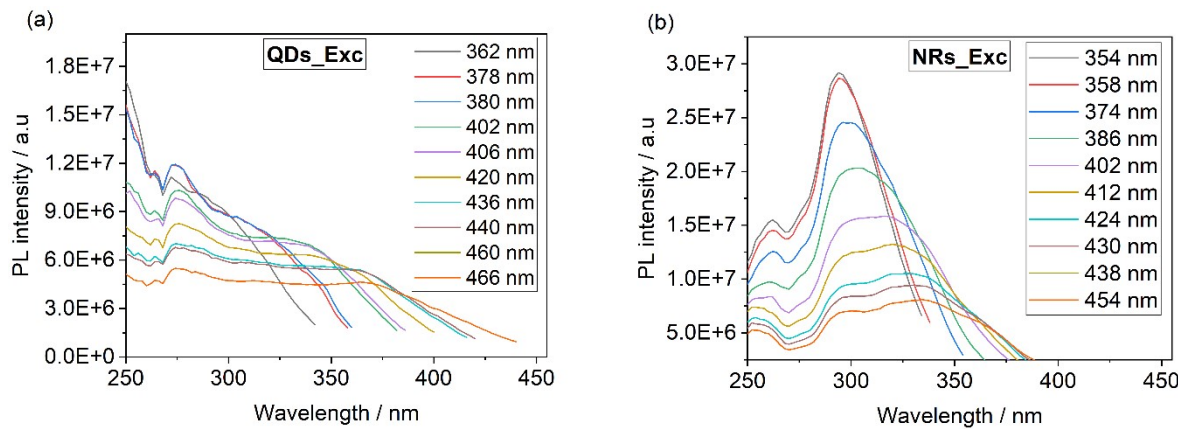


**Figure S2.** Photoluminescence excitation spectra of sample **1**(a) and sample **2** (b).

The emission spectra of samples **1** and **2**, as illustrated in Figure S3, exhibit a noticeable redshift. Specifically, for sample **1**, the emission shifts from approximately 360 nm to 460 nm, while for sample **2**, it shifts from around 350 nm to 450 nm.

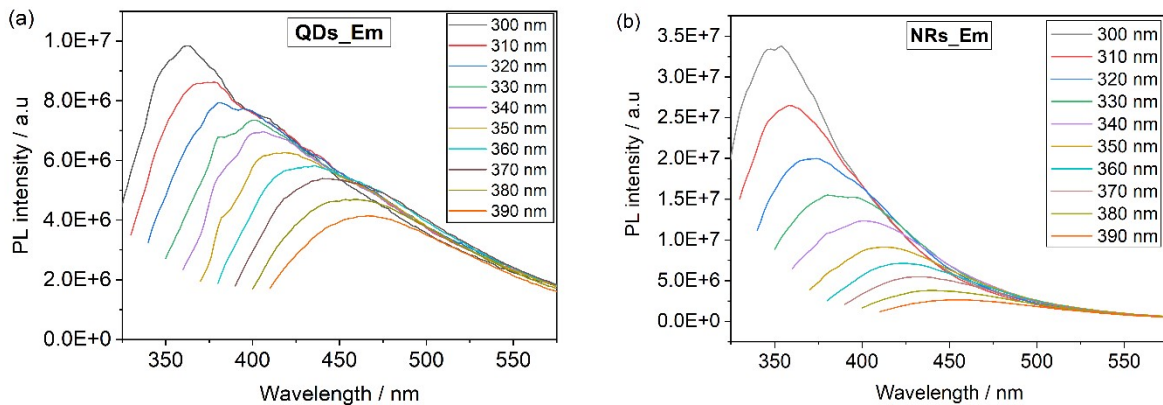


**Figure S3.** Photoluminescence emission spectra of sample **1**(a) and sample **2** (b)

For comparative analysis, Figure S4 presents a three-dimensional representation depicting the variations in emission spectra for samples **1** and **2**. This visual representation enables to discern alterations in intensity, peak positions, and spectral width for both samples.

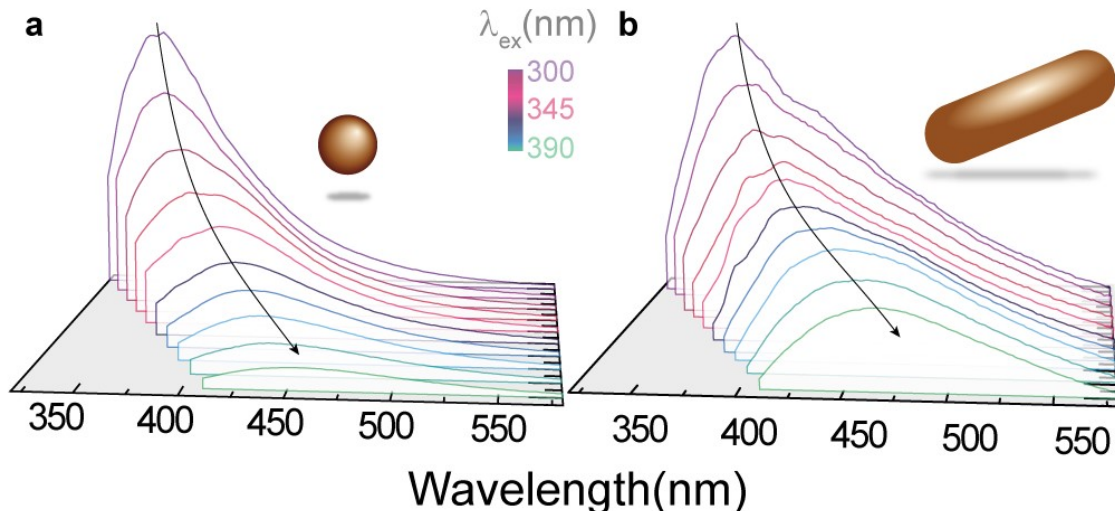


**Figure S4.** Emission spectra of **1** and **2** upon excitation at distinct wavelengths ( $\lambda_{\text{ex}}$ ) in polyethylene glycol 400 and oleylamine and ethanol respectively, at room temperature. The red shift of the emission peak with the increase of the excitation wavelength is due to the exciton fine structure.

### III. Thermal characterization

#### Variation of the photoluminescence with temperature

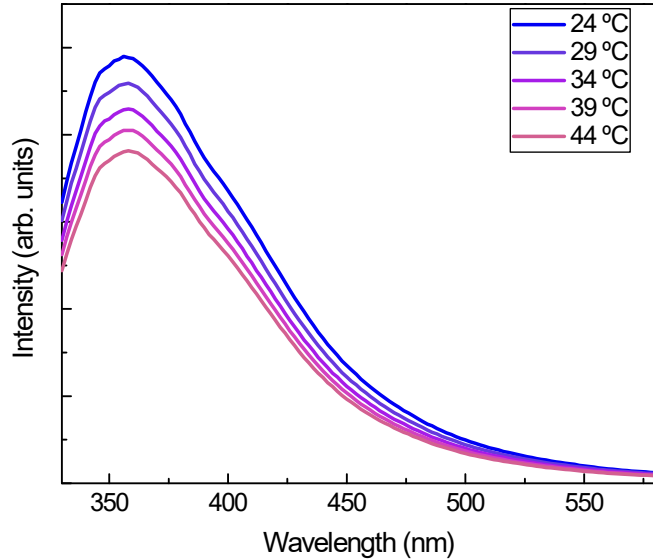


**Figure S5.** Emission spectra at different temperatures of **2** in ethanol.

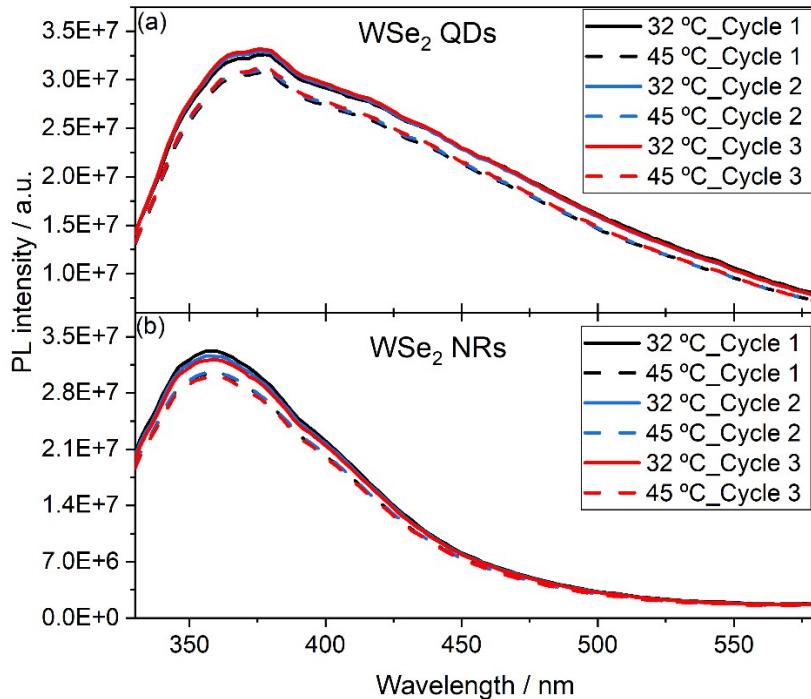


**Figure S6.** Emission spectra upon 310 nm excitation recorded in 3 temperature cycles for (a) **1** and (b) **2**.

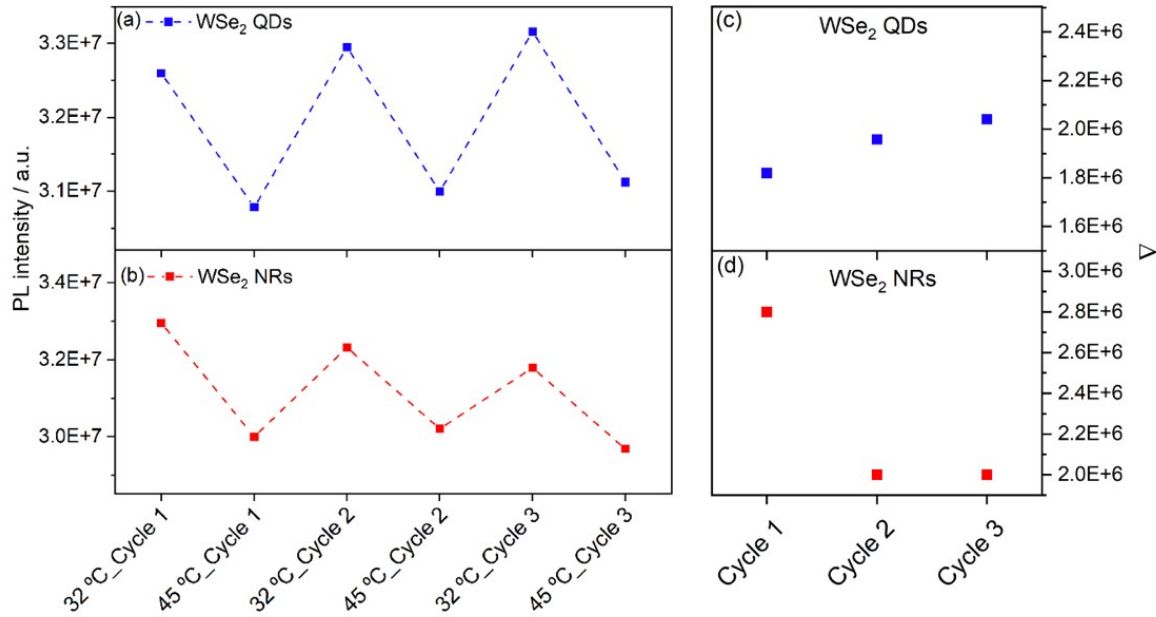


**Figure S7.** (a and b) Emission peak intensity emission during temperature cycles and (c and d)  $\Delta$ , variation of PL intensities between cycles.

**Fit parameters of the thermal calibration curves for the samples.**

The thermometric parameter  $\Delta = A_A/A_B$  follows a linear decreasing trend with temperature.

Table S2 shows the value of the variables obtained in the linear fit ( $y = a + bx$ ).

**Table S3.** Value of the intercepts (*a*), slopes (*b*) of the linear fit and  $r^2$ .

Sample	Thermometric Parameter	Variable	Value
<b>1</b>	$\Delta$	<i>a</i>	-0.2371± 0.035
		<i>b</i>	0.0016± 1.155
		$r^2$	0.98
<b>2</b>	$\Delta$	<i>a</i>	-0.7292± 0.123
		<i>b</i>	0.0043± 4.030
		$r^2$	0.96

**Table S4.** Deconvolution fit parameters at distinct temperatures (T) for **1**.

T (K)	Parameter						R <sup>2</sup>
	A <sub>A</sub> (±0.01)	A <sub>B</sub> (±0.01)	W <sub>A</sub> (±8 cm <sup>-1</sup> )	W <sub>B</sub> (±8 cm <sup>-1</sup> )	E <sub>A</sub> (±10 cm <sup>-1</sup> )	E <sub>B</sub> (±10 cm <sup>-1</sup> )	
297	0.396	0.680	1826	4477	27918	25954	0.995
305	0.369	0.666	1813	4390	27912	25983	0.992
307	0.349	0.662	1748	4394	27897	26075	0.993
312	0.344	0.649	1752	4362	27900	26053	0.996

**Survey on relative thermal sensitivity and temperature uncertainty in TMDCs, quantum dots and nanowires samples.**

**Table S5.** Comparison of thermal sensitivity and thermal uncertainty values from works found in the literature and in this work.

Material	Relative thermal sensitivity (% K <sup>-1</sup> )	Temperature uncertainty (K)	Obs.	Reference
ReS <sub>2</sub> Nanowalls	0.016	-	Peak position	<sup>1</sup>
N,S co-doped carbon Dots	0.64	-	Single intensity	<sup>2</sup>
PbS QD in glass	0.456	-	Intensity ratio	<sup>3</sup>
ZnS QDs	0.9	0.623		<sup>4</sup>
BiFeO <sub>3</sub> NWs	0.75	-		<sup>5</sup>
WSe <sub>2</sub> QDs ( <b>1</b> )	0.80	1.5	Intensity ratio	This work
WSe <sub>2</sub> QDs ( <b>1</b> )	30	0.1	MLR*	
WSe <sub>2</sub> NWs ( <b>2</b> )	0.66	1.7	Intensity ratio	

\* Multiple linear regression

**IV. References**

1. X. J. Xu, X. W. Hu, X. L. Li, M. M. Yang, J. T. Liu, Q. L. Guo, Y. Wang and B. L. Liang, *Nanotechnology*, 2021, **32**.
2. Z. Y. Guo, J. B. Luo, Z. P. Zhu, Z. S. Sun, X. G. Zhang, Z. C. Wu, F. W. Mo and A. X. Guan, *Dyes Pigments*, 2020, **173**.
3. Z. Wang, J. B. Li, F. F. Huang, Y. J. Hua, Y. Tian, X. H. Zhang and S. Q. Xu, *Journal of Alloys and Compounds*, 2023, **942**.
4. P. Conceição, J. F. Barata, M. A. Hernández-Rodríguez, P. S. Lacerda, M. G. Neves, L. D. Carlos and T. Trindade, *Sensors and Actuators A: Physical*, 2023, **357**, 114382.
5. K. Prashanthi, K. K. Mohan, Z. Antic, K. Ahadi and M. D. Dramicanin, *Micro Nano Syst Lett*, 2022, **10**.